Electrostatic turbulence intermittence driven by biasing in Texas Helimak

D. L. Toufen, F. A. C. Pereira, Z. O. Guimarães-Filho, I. L. Caldas, and K. W. Gentle

Citation: Physics of Plasmas (1994-present) **21**, 122302 (2014); doi: 10.1063/1.4903201
View online: http://dx.doi.org/10.1063/1.4903201
View Table of Contents: http://scitation.aip.org/content/aip/journal/pop/21/12?ver=pdfcov
Published by the AIP Publishing

Electrostatic turbulence intermittence driven by biasing in Texas Helimak

D. L. Toufen,[1,2] F. A. C. Pereira,[2] Z. O. Guimarães-Filho,[2] I. L. Caldas,[2] and K. W. Gentle[3]
[1]*Federal Institute of Education, Science and Technology of São Paulo - IFSP, 07115-000 Guarulhos, São Paulo, Brazil*
[2]*Institute of Physics, University of São Paulo, 05315-970 São Paulo, São Paulo, Brazil*
[3]*Department of Physics and Institute for Fusion Studies, The University of Texas at Austin, Austin, Texas 78712, USA*

(Received 30 June 2014; accepted 14 November 2014; published online 4 December 2014)

We investigate changes in the intermittent sequence of bursts in the electrostatic turbulence due to imposed positive bias voltage applied to control the plasma radial electric field in Texas Helimak [K. W. Gentle and H. He, Plasma Sci. Technol. **10**, 284 (2008)]—a toroidal plasma device with a one-dimensional equilibrium, magnetic curvature, and shear. We identify the burst characteristics by analyzing ion saturation current fluctuations collected in a large set of Langmuir probes. The number of bursts increase with positive biasing, giving rise to a long tailed skewed turbulence probability distribution function. The burst shape does not change much with the applied bias voltage, while their vertical velocity increases monotonically. For high values of bias voltage, the bursts propagate mainly in the vertical direction which is perpendicular to the radial density gradient and the toroidal magnetic field. Moreover, in contrast with the bursts in tokamaks, the burst velocity agrees with the phase velocity of the overall turbulence in both vertical and radial directions. For a fixed bias voltage, the time interval between bursts and their amplitudes follows exponential distributions. Altogether, these burst characteristics indicate that their production can be modelled by a stochastic process. © *2014 AIP Publishing LLC*. [http://dx.doi.org/10.1063/1.4903201]

I. INTRODUCTION

In toroidal magnetic fusion devices, the plasma edge turbulence limits the plasma confinement. The basic characteristics of edge turbulence are common to several fusion devices as tokamaks, stellarators, and reversed field pinches.[1–4] Complementary plasma turbulence and their statistical and spectral characteristics have been investigated in several simpler magnetic plasma devices.[5–11] The comparison of the structure of fluctuations supports that plasma turbulence displays universal characteristics common to all these devices.[12,13]

Generally, such observed turbulence in the density fluctuations consists of two components: a broad band background fluctuation and a sequence of large intermittent bursts. These bursts are encountered in the edge and the scrape-off-layer (SOL) of tokamaks, stellarators, reversed field pinches, and also in other magnetized devices.[5,7,8,11–15] In particular, a significant fraction of the total transport to the walls in all of these devices can be attributed to the presence of large and sporadic bursts.[14,16]

Thereupon, several procedures have been tried to control plasma turbulence and improve the confinement in fusion devices. Experiments in the Reverse Field pinch eXperiment (RFX) at padua showed turbulence changes with external radio frequency (RF) wave amplitude,[17] by launching waves using two electrostatic probes in the shadow of the limiter,[18] or by imposing an external electric potential that changes the radial electric field profile.[19–21]

Recently, several experiments have also been performed to study electrostatic turbulence in plasmas with flow and magnetic shear in helimaks.[22–26] The helimak is one of a class of basic plasma experiments with characteristics of fusion plasmas in a simple geometry. This basic plasma toroidal device has a sheared cylindrical slab that simplifies the turbulence description and provides results that can be used to understand the plasma edge and the scrape-off layer in major fusion machines.[27] As the plasma of helimak is colder and less dense when compared with tokamaks, it is possible to use a large set of diagnostic probes. These characteristics make the helimak an interesting device to study the plasma flow shear influence on wave turbulence.[23,29]

In Texas Helimak, for negative biasing, turbulence control has been investigated and states of greatly reduced turbulence have been achieved.[22,28] Furthermore, it was found evidence that induced transport turbulence in this device is much affected by wave particle resonances and, eventually, by a kind of shearless transport barrier.[30] On the other hand, for positive biasing, previous experiments in Texas Helimak support that for positive biasing, turbulence shows enhanced broadband spectra and nonGaussian Probability Distribution Function (PDF) with extreme events.[31]

In this article, we analyze a new set of measurements recently performed in Texas Helimak, on turbulence broadband spectra enhanced by positive biasing, to investigate how the occurrence of bursts and their propagation change with the alterations on the radial electric field profile. For that, we consider a plasma region with roughly uniform equilibrium gradients, compelled by external positive voltage bias applied to a set of border plates. We analyze the ion saturation fluctuations in these perturbed discharges, collected in a large set of Langmuir probes available at the Texas Helimak, and identify characteristics of the intermittent burst propagation and their dependence on the applied bias potential.

The observed turbulent signals have two components: the almost stationary nearly Gaussian random fluctuations and the intermittent bursts, similar to what has been observed in many experimental investigations of turbulence in several magnetic confinement devices.[14,16] We identify the intermittent bursts and determine the distribution of their amplitude, which follows an exponential decay. We also found an exponential distribution of the time interval between successive bursts, suggesting a process formation independent of their eventual predecessors. We also determine the burst characteristics by the self and cross conditional average method and the burst propagation velocity. Thus, we identify bursts propagating along the plasma flow with velocities close to the broadband turbulence phase velocity.

The number of bursts increase with positive biasing, giving rise to a long tailed skewed turbulence probability distribution function. The burst shape and amplitude do not change much while the burst vertical velocity increases monotonically with the applied bias voltage. Furthermore, for the highest bias voltage values, the bursts vertical velocity (corresponding to the poloidal velocity in the tokamak case) is much higher than their radial velocity.

In Sec. II A, we review the experimental set up. In Sec. II B, we describe the turbulence perturbed by a positive bias voltage in Texas Helimak, the observed extreme events in Sec. III and, in Sec. IV, the influence of the positive external biasing on the intermittent bursts. Finally, in Sec. V we comment on our main conclusions.

II. TEXAS HELIMAK

A. Experimental set up

The experiments were recently performed at Texas Helimak,[22] a basic plasma toroidal device located at the University of Texas at Austin. In this machine, the combination between the toroidal and the small vertical field creates a helical magnetic field with curvature and shear as shown in Fig. 1. Texas Helimak has a vacuum vessel with rectangular cross section of external radius $R_{external} = 1.6\,\text{m}$, internal radius $R_{internal} = 0.6\,\text{m}$, and height $H = 2\,\text{m}$. Most of these magnetic field lines start and terminate into four sets of four plates located at the top and the bottom part of the machine. These plates are used as a support to the Langmuir probes and to apply external electric potentials (bias) to change the radial electric field profile. The Helimak geometry is well described by the sheared cylindrical slab[27] since the connection lengths are long enough to neglect the end effects.

In Texas Helimak, the turbulence can be modified by changing the radial profile of the electric potential, and thus, changing the radial electric field component. This electric field alteration can be achieved by imposing an external electric potential on some of the 16 available bias plates (see Fig. 1(a)). For a normal grounded operation, all the plates are connected to the vessel ground. An equilibrium electric potential results from the sheath boundary conditions, resulting in vertical, sheared $E \times B$ flows.[28] For the biased operation, the plates within a chosen radial range are connected to a bias voltage. This bias induces a radial electric field that

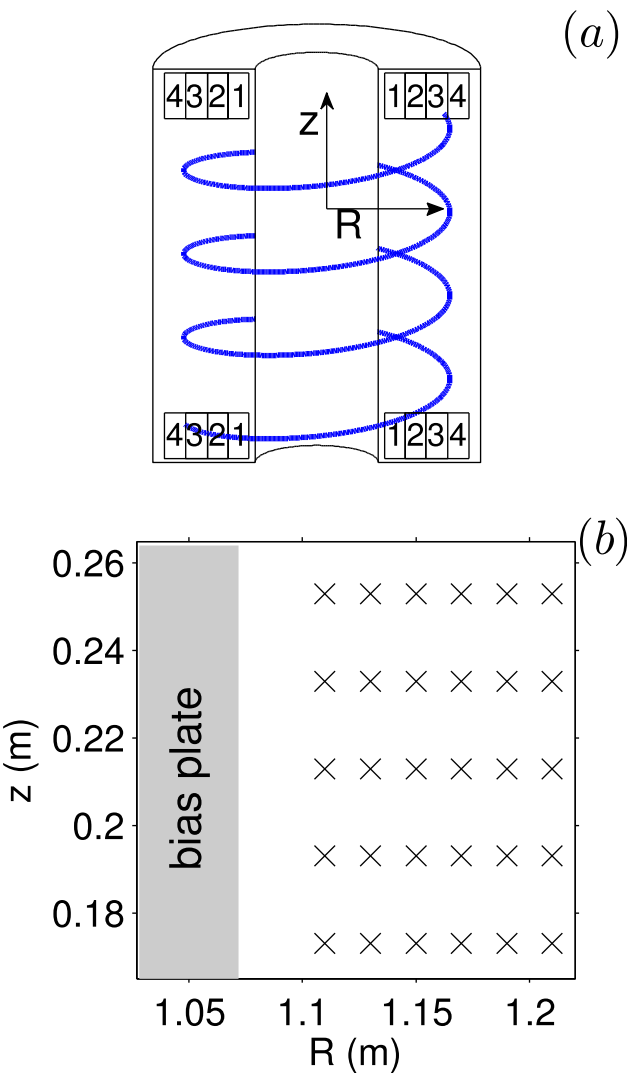

FIG. 1. Schematic of the Texas Helimak with a sample magnetic field line (a). Position of the main Langmuir probes considered in this work (b). Grey region indicates part of the bias plate.

can strongly impact the potential profile and the vertical $E \times B$ flows.

In the analyzed experiments, the dominant toroidal field is about 0.1 T. For the experiments analyzed in this work, Argon gas at 10^{-5} Torr was heated by electron cyclotron resonance heating with 6 kW of power inserted by a window located in the inner side of the vacuum vessel, located around $R = 0.95\,\text{m}$ (where the bias plates are located). The shot duration is up to 20 s, and the plasma is in a steady state with stationary conditions during at least 10 s, the time interval considered for fluctuation analyzes described in this work. Electrostatic probes mounted at the four sets of bias plates were used to measure saturation current fluctuations analyzed in this work and data were taken by two digitizers, one with 96 channels and 500 kHz of sample rate and another one with 128 channels and 7 kHz of sample rate for mean profiles.

For the shots analyzed in this paper (130128005–130130024), bias is imposed in the four plates (two on the top and two on the bottom, on both sides of the machine, labelled by the numbers 2 in Fig. 1 placed in the interval from

$R > 0.86$ m to $R < 1.07$ m) near the radial region chosen to analyze the turbulence ($1.10\,\text{m} < R < 1.15\,\text{m}$). Data presented in this paper are obtained from a set of probes place in the bottom of the machine in the plate by the number 3, at the same toroidal position of the bias plates (Fig. 1(b)). In this region, the density gradient is practically uniform and the electric field is much affected by the external bias.

B. Intermittent turbulence

In Helimak the turbulence changes due to alterations on the radial electric field imposed by the applied voltage potential. In fact, data analyzes showed two different kinds of perturbed turbulence. Overall, the turbulence level is reduced for negative biasing.[22,28,31] However, for positive biasing the turbulence shows enhanced broadband spectra and nonGaussian PDF with intermittent extreme events,[31] as it is briefly presented in this section. The main introduced spectrum characteristics, shown in Figures 2 and 3, are those required to follow the new results, presented in Secs. III and IV, on the intermittent burst propagation and their dependence on the applied positive bias potential.

In this work, we consider time intervals about 9.7 s for current saturation time series $I_{sat}(t)$, obtained for each probe used in the configuration, to perform statistical and spectral analyses of the plasma turbulence. For the spectral analysis, we perform a windowed Fast Fourier Transform (FFT) algorithm dividing the data time series into 194 series with 25×10^3 points each.[31]

Figure 2 shows an example of a saturation current signal, part of the time series for fluctuating ion saturation current perturbed by a bias potential of 10 V, measured in a probe located at $R = 1.13$ m and $z = 0.233$ m ($z = 0$ on the bottom). High intensity spikes can be easily distinguished.

The turbulent fluctuation distribution functions of different devices have significant non-Gaussian features. In particular, a significant fraction of the total flux can be attributed to the presence of large and intermittent bursts.[12,13] Likewise, the PDF of the I_{sat} signal of the turbulence observed for positive biasing, showed in Fig. 2(c), have a long tail, an indication of intermittent bursts. The kurtosis and skewness are higher than the values $K = 3$ and $S = 0$ obtained for Gaussian distributions, indicating the presence of positive extreme events much more common than what is expected from a random distribution. Namely, this deviation from a Gaussian is due to the presence of intermittent bursts. The same kind of PDF with long tail is been commonly observed in tokamak scrape-off layers and other devices, combined with a great variability in the amplitude of bursts as well as in the time interval between two successive bursts.[12,14,32,33] Thus, our observations confirm that the analyzed signals possess the two usual components: a random nearly Gaussian fluctuations plus intermittent bursts.[12,34]

An example of power spectra, for the signal of Fig. 2, is shown in Fig. 3(a). This spectrum shows that energy of the signal is concentrated in the interval $0.1\,\text{kHz} < f < 1\,\text{kHz}$. The coherence spectra between two probes in the same radial position, Figure 3(b), show a high coherence for $f < 3$ kHz.

To better characterize the fluctuations, we also present the $S(k,f)$ spectrum, obtained from two probe measurements

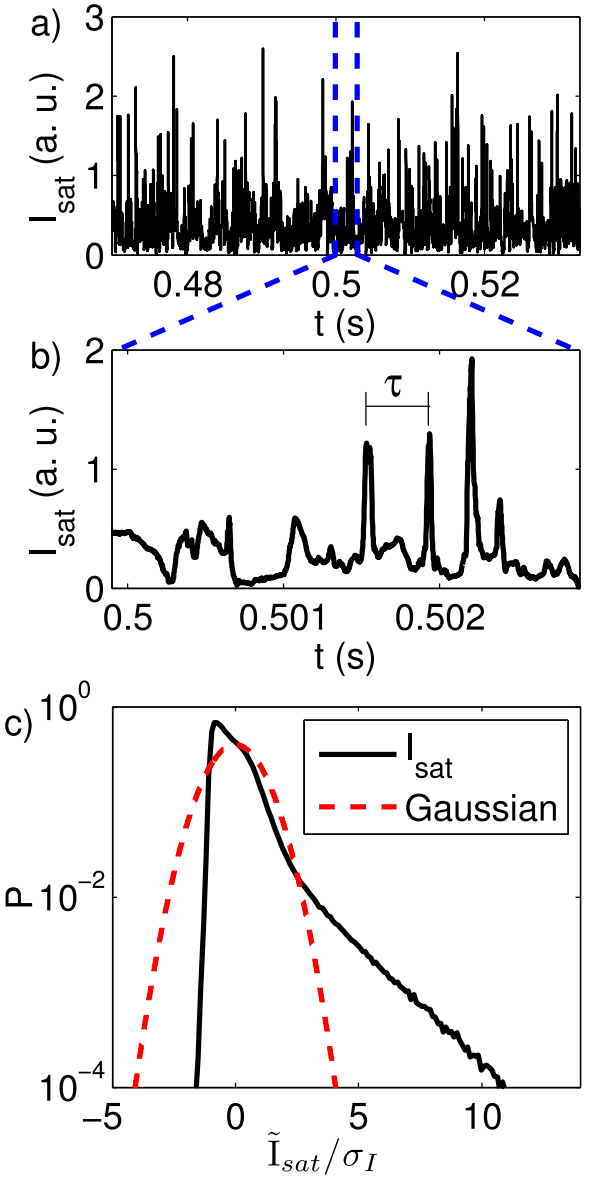

FIG. 2. Saturation current signal shown in a small time interval (a) and a zoom in (b). Signal obtained for R = 1.13 m, z = 0.233 m and a bias voltage of 10 V. PDF of the complete saturation current signal (c). A Gaussian distribution is shown with the dashed line for comparison.

as the bidimensional histogram of the amplitudes of the cross spectrum in terms of the wave number and frequency among several similar realizations.[35] The $S(k,f)$ spectrum is observed in Fig. 3(c), in which we present in color scale the obtained signal power as a function of its frequency and wave number. The frequency spectrum is broad and shows an average linear dependence $k(f)$ so, even without a mode with a well determined frequency, the average phase velocity, estimated through this spectrum,[36] is the same for all frequencies. So, this spectrum presents an important characteristic: all the waves in the turbulence spectrum have the same phase velocity, what is not commonly observed in broadband turbulences.

III. EXTREME EVENTS

In this section, we analyze the burst form, their frequency, and how they propagate in the plasma. In particular,

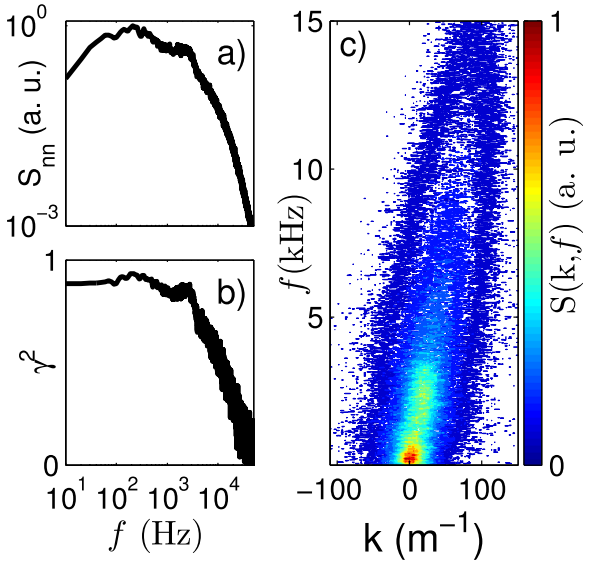

FIG. 3. Power spectrum (a) of the signal obtained for R = 1.13 m, z = 0.233 m, coherence spectrum (b) and S(k,f) spectrum between signals of probes positioned in z = 0.213 m and 0.233 m, R = 1.13 m and bias = 10 V.

we obtain the burst amplitude and their waiting time distributions which could reveal the statistical nature of the extreme events. We also use conditional analysis to identify the mean shape of bursts propagating in the plasma.

Initially, for data from probes at $R = 1.11$ m and a shot with a bias voltage of 10 V, we present in Fig. 4(a) the probability distribution of burst amplitudes, $P(A)$, normalized by the standard deviation, σ_I, of the entire time series. In this figure, we see that the distribution of number of bursts as a function of their normalized amplitude can be well represented by an exponential fitting, $P(A) = Ce^{(-A/A_0)}$.

Another important issue is the distribution of time between intermittent events.[5,37,38] Once the bursts instants are detected, we determine the time between two consecutive bursts, τ, and its PDF. Accordingly, for the same data used for Fig. 4(a), from probes at $R = 1.11$ m and a shot with a bias voltage of 10 V, we present in Fig. 4(b) the probability distribution, $P(\tau)$, of time intervals, τ, between two successive bursts (considering events with amplitude equal or higher than three times the standard deviation). This probability distribution has an exponential decay, $P(\tau) = De^{-\tau/\tau_0}$, the same exponential distribution observed for the inter bursts time of the intermittent fluctuation in the tokamak scrape-off layer.[14] The amplitude and time between bursts distributions can be interpreted as evidences of the stochastic nature of the observed intermittence. Specially for $P(\tau)$ in which exponential distribution is a consequence of an uniform burst appearance probability.[39]

In order to investigate the bursts propagation, we performed a coincidence analysis in nine neighbor probe fluctuations data. Delay time histograms are obtained by counting the time intervals relative to the time in which the peak of the burst is identified at the reference probe (in the center of Fig. 5). As the mean time interval between successive bursts is much higher than the burst propagation time from one probe to the other, the computed time delay measurements have a good resolution. The red lines in Fig. 5 represent the

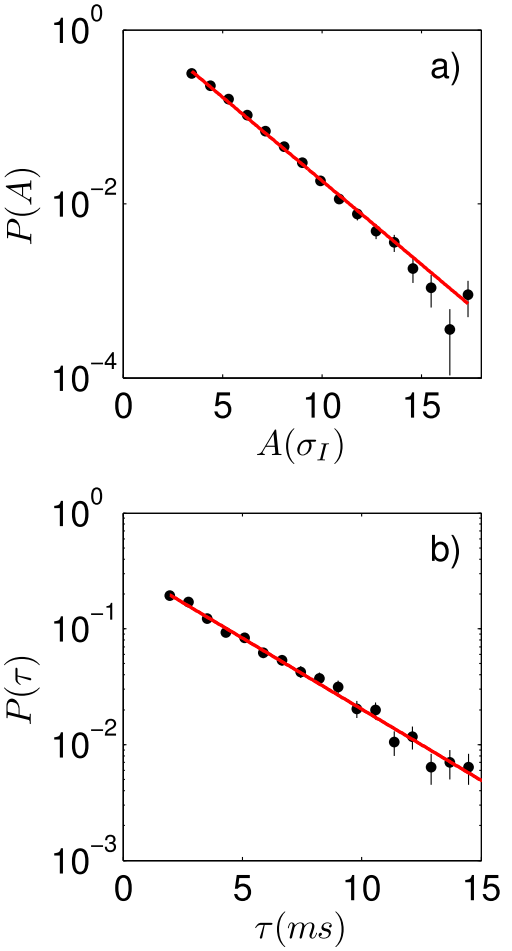

FIG. 4. (a) Probability distribution P(A) of the burst amplitudes. The amplitude A is normalized by the standard deviation σ_I of the entire time series. (b) Probability distribution P(τ) of the time interval between two consecutive bursts. On this discharges bias = +10 V and the analyzed probe was located at R = 1.13 m and z = 0.213 m.

function, a Gaussian plus a constant, adjusted for the time delay distribution. In conclusion, in Fig. 5, the histograms of extreme events in one probe in time coincidence with an extreme event detected in the reference probe shows a higher dispersion for probes with the same vertical position and different radial positions in comparison with dispersion for probes with same radial position and different vertical positions. This means that the bursts propagation is better defined in the vertical than in the radial direction.

Once the coincidence histograms of Fig. 5 made the bursts propagation evident, we consider the conditional averaging technique to follow the statistical evolution of selected conditions in the signal. Thus, Figure 6(a) shows cross conditional average between the I_{sat} signal of a probe positioned at $R = 1.13$ m and $z = 0.213$ m and the signals from two neighbour probes with the same vertical position. Figure 6(b) shows the conditional average between the signal from the same reference probe and four probes below and above at the same radial position. From Fig. 6, we see that these cross conditional average results confirm that the bursts are propagating preferentially in the vertical direction, as inferred from the histograms of Fig. 5. The observed resemblance of the cross correlations from signals in equidistant probes is an

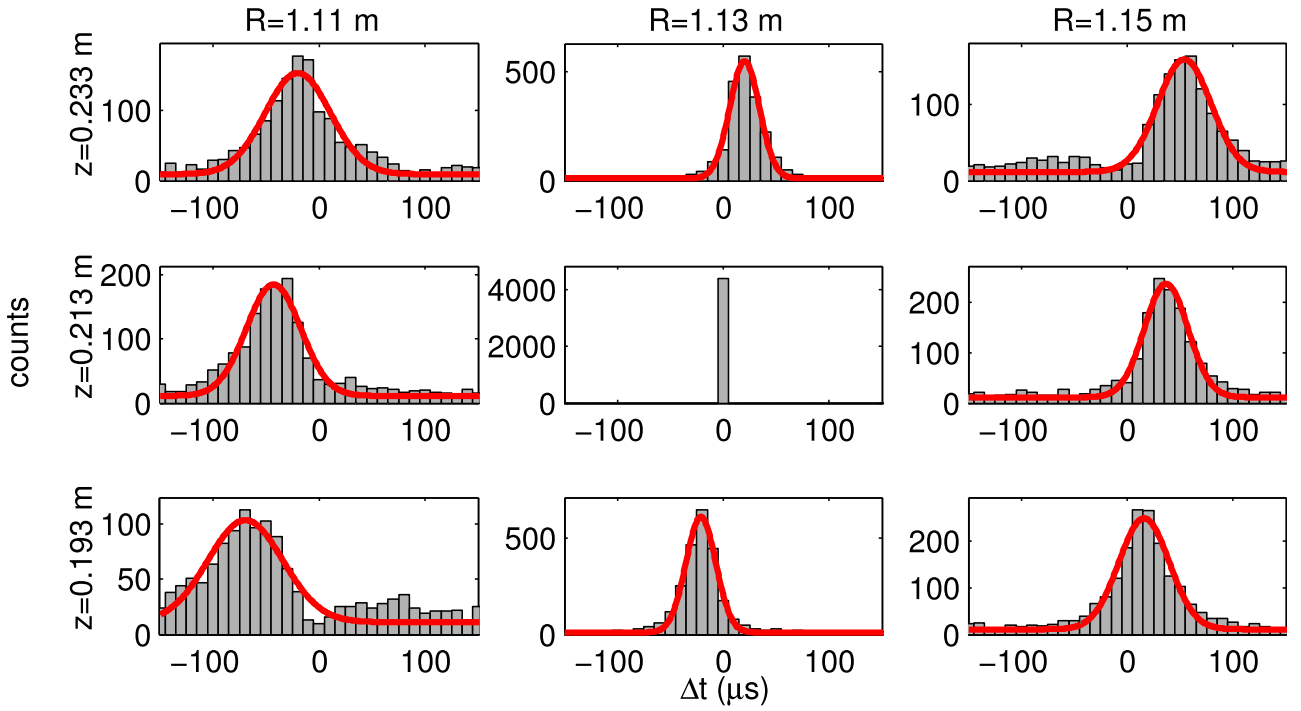

FIG. 5. Histograms of extreme events with time coincidence with the extreme events identified in a reference probe (R = 1.13 m and z = 0.213 m). The line is a Gaussian plus background adjust. On this discharges bias = +10 V.

evidence of the bursts propagation with uniform velocity along the probe separation in the vertical (z) and radial (R) directions.

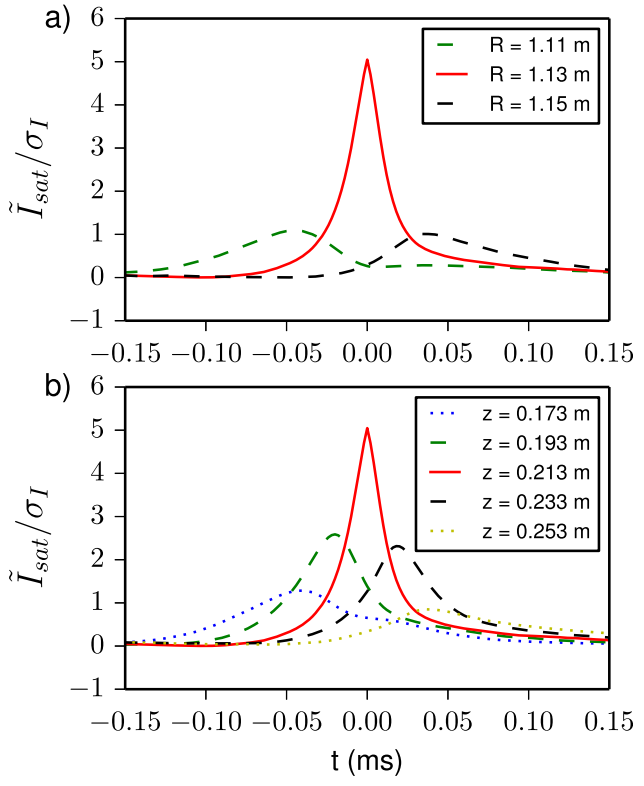

FIG. 6. (a) I_{sat} signal cross-conditional average along the radial direction for z = 0.213 m. (b) I_{sat} signal cross-conditional average along the vertical direction for R = 1.13 m. The reference probe is positioned at R = 1.13 m and z = 0.213 m and bias = +10 V.

Observing Fig. 6, we note that the burst shape obtained from the conditional average is spread enough to be observed in more than one probe. Indeed, for a discharge with $+10\,V$ of bias voltage the Fig. 7 shows the bidimensional burst shape, in three time frames, where the conditional average levels are indicated through the color scale. Thus, we can identify the bursts propagation in both the vertical and radial direction. The two-dimensional conditional average has also been used in LArge Plasma Device (LAPD)[11] to investigate the propagation of structures associated to strongly intermittent turbulence in the shadow of a limiter in LAPD, a linear magnetized plasma with a steep density gradient.

In order to determine the burst velocities, we perform a bidimensional fit which takes into account a set of time frames to estimate the burst size and his peak velocity. This fitting, explained in detail in the Appendix, assume constant velocities for the burst peak in both vertical and radial directions. The black contour lines indicated in Fig. 7 are obtained from the fitted functions. This procedure is used to avoid overestimation of the burst velocities that could be obtained by only considering the time delays between orthogonal probes. This overestimation would result from the elongated and tilted burst shape mentioned in the next paragraph. This difference between the apparent burst velocity inferred from time delays and the real propagation velocity of the burst structure is one of the important contributions of the analysis presented in the paper, which only could be carried out because of the large set of close Langmuir probes of Texas Helimak.

From the adjust shown in Fig. 7 is clear that the bursts are tilted and elongated structures with largest characteristic length about 6 cm. The tilt is approximately 60° with radial direction and the ratio between the smallest and the largest characteristic lengths is about 1/4.

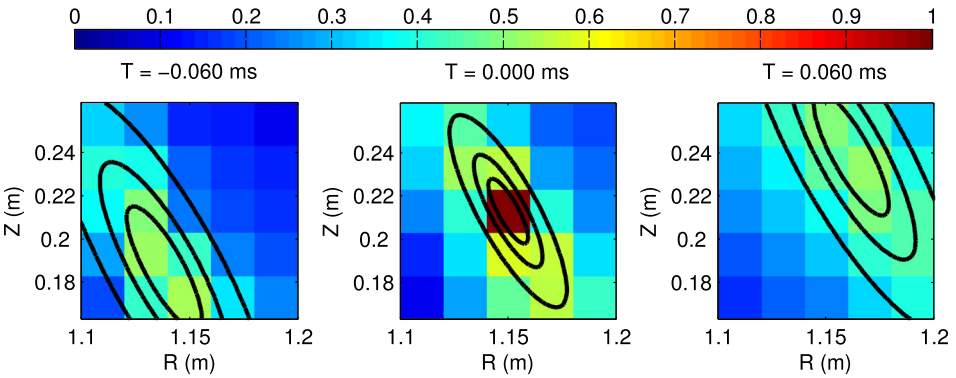

FIG. 7. Relative amplitude of the cross-conditional average for a set of probes and three different relative times. The black lines are the contour of the bidimensional adjust. On this discharges bias = +10 V.

Besides their stochastic nature, we have not yet determined the mechanism of burst creation. Even so, we determine their structure and how they propagate in the plasma. The burst driving mechanism has been investigated in other machines. In TORPEX, a device similar to Texas Helimak, it was found that the blob creation is related to the magnitude of the temporary density gradient that induces coherent waves in a inner radial region.[40,41] However, in our analyzed discharges no evidence of coherent waves driving bursts has been found. Furthermore, our analyzes could be considered as complementary to the TORPEX observations of propagating blobs in uniform density regions, as we describe bursts propagating in the uniform gradient density radial region. The two different density profiles regions analyzed in Texas Helimak and TORPEX are similar to the tokamak density profiles, at the plasma edge and in the scrape-off layer, respectively, and may drive different bursts propagations as those observed in the two tokamak regions.

IV. BIAS DEPENDENCE

Experiments with bias voltage to investigate the bursts control have been performed in Texas Helimak[22,28] and TORPEX.[42] In this section, we examine how the burst shape and burst waiting time change with the bias voltage.

Initially, we present Fig. 8 with three average saturation current radial profiles for three bias voltage values, From this figure, within our approximation, we can consider that the equilibrium density radial profile does not change much with

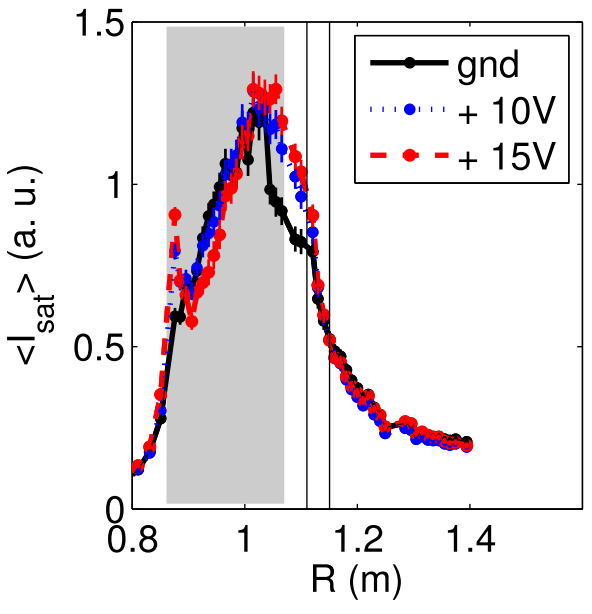

FIG. 8. Radial profiles of the mean saturation current for three different bias values: ground (solid black line), +10 V (doted blue line), and +15 V (dashed red line). This profiles are directly related with the mean densities profiles. Grey region indicates the radial region of the bias plates.

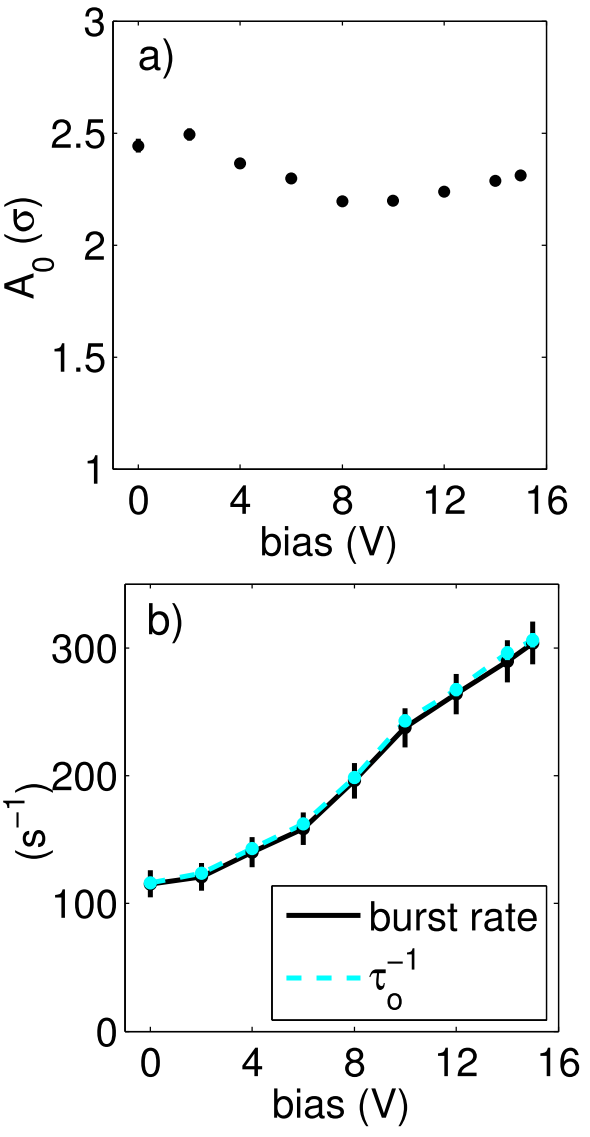

FIG. 9. (a) Characteristic amplitude decay. (b) Bursts rate and characteristic time decay, τ_0^{-1}, as a function as bias values for four probes placed at R = 1.13 m and z = 0.253, 0.233, 0.213 and 0.193 m.

the bias voltage, especially in the marked radial interval where our turbulence data is collected for the presented analysis. Thus, as the density gradient remains approximately constant for different applied bias voltage values, the turbulence changes can be mainly attributed to the bias radial electric field control.

To investigate the effect of bias in the amplitude of the bursts we use the fitting shown in Fig. 4 to calculate the amplitude decay coefficient, A_0, as a function of the bias value for a fixed radial position, $R = 1.13$ m. As observed in the Fig. 9(a), A_0 presents a weak dependency with bias values. The conditional analysis revels that not only the burst amplitude but also its shape remains unchanged as the applied bias voltage increases.

In addition, we verify the effect of bias value in the bursts abundance by calculating the burst rate, represented by the solid curve in Fig. 9(b), as the registered number of bursts divided by the observation time interval. Complementary, this same figure also shows, in a dashed curve, the coefficient τ_0^{-1} of the distribution $P(\tau) = Ce^{-t/\tau_0}$ (see Fig. 4(b)). Comparing these two curves, we observe that the measured burst rate agrees with the average value obtained from the previous PDF distribution, confirming our $P(\tau)$ fitting. Moreover, Figure 9 clearly shows that increasing bias voltage monotonically increases the number of bursts per second from 100 to 300.

Finally, we present in Fig. 10 the radial and vertical components of the burst and phase velocities and their dependence on the applied bias voltage. The phase velocities are calculated from the average wave number and frequency obtained from $S(k,f)$ spectra for fluctuations in pair of probes. The bursts velocities are close to the average phase velocities and they increase monotonically with the bias voltage. In fact, we expect the plasma potential and also the radial electric field change with the biasing and, consequently, the vertical ExB drift velocity. Indeed, optical measurements of the radial profile of the vertical flow velocity show modifications with the bias that follows the expected changes on the ExB drift velocity.[28] In a bias voltage range of 15 V, the radial velocities increase by a small amount while the vertical velocities triplicate their values. Therefore, for the highest bias values the bursts propagate mainly in the vertical direction.

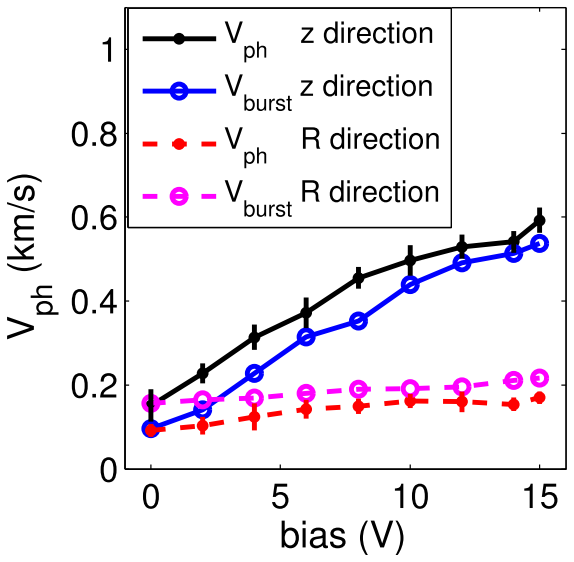

FIG. 10. Phase velocity (filled dots) and burst center velocity (empty dots) in vertical (solid lines) and radial (dashed lines) directions. The uncertainty of the bursts velocities is smaller than the size of the empty dots.

V. CONCLUSIONS

We investigated changes in the intermittent sequence of bursts in the electrostatic turbulence due to imposed positive bias voltage applied to control the plasma radial electric field in Texas Helimak. We identified the burst characteristics by analyzing ion saturation current fluctuations collected in a large set of Langmuir probes. To investigate the intermittence changes, we analyzed data from a set of discharges with chosen probe positions and a sequence of bias voltages, appropriate to determine the burst shape and burst propagation in plasma.

The performed statistical analysis shows a monotonic increase in the number of bursts, with approximately constant amplitude distribution, with the external bias voltage. This is a noticeable result once the plasma vertical velocity shear increases with the external bias voltage and, in the framework of the shear reduction turbulence models, one would expect a reduction on the amount of large structures when the velocity shear increases.

For a fixed bias voltage, the distribution of the burst amplitude distribution decays exponentially and the exponential decay rate does not change much with the applied bias voltage. The time interval between consecutive bursts also follows an exponential distribution, which decay decreases with the bias voltage, suggesting a formation process independent of the preceding bursts. These reported exponential decays support a stochastic model for the analyzed bursts as the one recently proposed.[39] Furthermore, from the statistical point of view, the reported bursts average shape and PDFs of time between bursts and amplitudes present similar behaviour of bursts in tokamak scrape-off layer.

In order to investigate the bursts propagation in the radial and vertical directions (the vertical direction corresponds to the poloidal direction in tokamaks), we applied the data probe conditional analysis. Analyzing the cross-conditional averages, through a bidimensional adjust, we estimate the burst peak velocity and found it close to the fluctuation average phase velocity, unlike commonly observed in Tokamaks. These peculiar close velocities and their similar monotonic increasing with the applied bias voltage could be explained by the burts predominance in the examined turbulence regime. The bursts vertical velocity (corresponding to the poloidal velocity in the tokamak case) increases significantly with the bias voltage becoming much higher than the radial velocity.

In conclusion, several key characteristics are presented of the burst propagating in a sheared plasma flow and their dependence on the radial electric field. Furthermore, the reported characteristics may contribute to understand the burst properties observed in other experiments in fusion and nonfusion plasma devices.

ACKNOWLEDGMENTS

We would like to thank the discussions with Professor W. Horton JR (The University of Texas at Austin, USA), the comments of Dr. M. V. A. P. Heller (University of São Paulo, Brazil), and the partial support of this work by the Brazilian agencies FAPESP (Processes 2012/22108-5 and 2011/19296-1), CNPq, and CAPES.

APPENDIX: BURST PROPAGATION MODEL

The typical one-dimensional (1D) cross-conditional averages presented in (Fig. 6) suggests that the burst is propagating in both vertical and radial directions. However, in the bidimensional (2D) cross-conditional averages presented in Fig. 7, it is possible to see that the average burst structure is tilted, which implies that the radial and vertical propagation of the peak position will be mixed when detected by the 1D cross-conditional averages. Therefore, in this Appendix we present the procedure used to estimate the radial and vertical velocity components, v_R and v_Z, of the burst peak from the 2D burst propagation shown in Fig. 7. To do that, we use the cross conditional averages on a 5×5 grid of probes, using the instants of the burst occurrence on the central probe as a reference. The chosen reference probe is the one at $R_r = 1.15\,\text{m}$ and $Z_r = 0.213\,\text{m}$.

We consider that in a given time frame t, the signal in the probe located at radial position R and vertical position Z can be described as

$$I_{sat}(R,Z,t) = I_F + I_B(t).F(R,Z,t)\,, \tag{A1}$$

where I_F is the average ionic saturation current, $I_B(t)$ is the amplitude of the burst peak at time t, and $F(R,Z,t)$ is the burst characteristic shape. In order to describe the experimental data, the burst characteristic shape must be a 2D titled peak with very different characteristics lengths. By defining the two orthogonal directions $\vec{e_1} = (\cos\theta,\ \sin\theta)$ and $\vec{e_2} = (-\sin\theta,\ \cos\theta)$ of the peak shape in which the characteristic lengths are s_1 and s_2, with $s_1 > s_2$, the peak shape can be written as

$$F(R,Z,t) = \frac{1}{1 + \left[\dfrac{(R - R_0(t))\cos\theta + (Z - Z_0(t))\sin\theta}{s_1(t)}\right]^2 + \left[\dfrac{(Z - Z_0(t))\cos\theta - (R - R_0(t))\sin\theta}{s_2(t)}\right]^2}\,, \tag{A2}$$

where $R_0(t)$ and $Z_0(t)$ are the radial and vertical positions of the peak and θ is the tilted angle. Equations (A1) and (A2) can be used to fit the 2-D peaks, but they will be seven parameters to be fitted $(I_F,\ I_B(t)\,, R_0(t)\,, Z_0(t)\,, s_1(t)\,, s_2(t)\,, \theta)$ in each time frame. In this case, the radial and vertical velocities can be estimated from the evolutions of the corresponding peak positions, $R_0(t)$ and $Z_0(t)$.

A further improvement in the fit can be done by imposing some constrains on the time evolution of the parameters. Indeed, the temporal evolutions of $R_0(t)$ and $Z_0(t)$ can be related with the corresponding peak velocities by $R_0(t) = R_r + v_R t$ and $Z_0(t) = Z_r + v_Z t$. Also, observing Figs. 6 and 7, we note that the amplitude of the peak decreases as the burst moves away from the reference probe, and the structure width increases. The amplitude decay indicates that the burst has a limited lifetime. The increase of the structure width could be explained by a diffusion of the burst or by the conditional averaging of bursts with slightly different velocities. In order to take in account these two effects, we consider that the amplitude decays exponentially with the time

$$I_B(t) = I_0 e^{-\mu|t|}\,, \tag{A3}$$

and the square of the characteristic lengths grow linearly

$$s_1(t) = \sqrt{s_0^2 + \delta|t|}\,. \tag{A4}$$

Furthermore, we assume that the ratio between the two characteristic lengths does not changes with the time, so $s_2 = \lambda s_1$, where $0 < \lambda \leq 1$. By using these constrains, it is possible to fit all time frames together using only nine parameters: $(I_F,\ I_0\,, \mu\,, v_R\,, v_Z\,, s_0\,, \delta\,, \lambda\,, \theta)$.

To obtain the burst velocity components (v_R and v_Z) present in Fig. 10 from the cross-conditional average for the 5×5 probe grid data, with the described procedure, we estimate the introduced parameters by using a least squares fitting. The nine parameters of the fitting reproduces quite well the conditional average evolution obtained from the data and gives the desired velocity components. An illustration of the fitted conditional average values is represented by the black contour lines in Fig. 7.

[1]C. Hidalgo, Plasma Phys. Control. Fusion **37**, A53 (1995).
[2]K. W. Gentle, Rev. Mod. Phys. **67**, 809 (1995).
[3]S. J. Zweben, J. A. Boedo, O. Grulke, C. Hidalgo, B. LaBombard, R. J. Maqueda, P. Scarin, and J. L. Terry, Plasma Phys. Control. Fusion **49**, S1–S23 (2007).
[4]W. Horton, Rev. Mod. Phys. **71**, 735 (1999).
[5]V. Antoni, V. Carbone, E. Martines, G. Regnoli, G. Serianni, N. Vianello, and P. Veltri, Europhys. Lett. **54**, 51 (2001).
[6]M. S. Baptista, I. L. Caldas, M. V. A. P. Heller, and A. A. Ferreira, Phys. Plasmas **10**, 1283 (2003).
[7]J. A. Boedo, D. Rudakov, R. Moyer, S. Krasheninnikov, D. Whyte, G. McKee, G. Tynan, M. Schaffer, P. Stangeby, P. West, S. Allen, T. Evans, R. Fonck, E. Hollmann, A. Leonard, A. Mahdavi, G. Porter, M. Tillack, and G. Antar, Phys. Plasmas **8**, 4826 (2001).
[8]Y. H. Xu, S. Jachmich, R. R. Weynants, and the TEXTOR team, Plasma Phys. Control. Fusion **47**, 1841 (2005).
[9]M. Farge, K. Schneider, and P. Devynck, Phys. Plasmas **13**, 042304 (2006).
[10]A. Vannucci, I. C. Nascimento, and I. L. Caldas, Plasma Phys. Control. Fusion **31**, 147 (1989).
[11]T. A. Carter, Phys. Plasmas **13**, 010701 (2006).
[12]G. Y. Antar, S. I. Krashennikov, P. Devynck, R. P. Doerner, E. M. Hollmann, J. A. Boedo, S. C. Luckhardt, and R. W. Conn, Phys. Rev. Lett. **87**, 065001 (2001).
[13]E. Sánches, C. Hidalgo, D. López-Bruna, I. García-Cortés, R. Balbín, M. A. Pedrosa, B. van Milligen, C. Riccardi, G. Chiodini, J. Bleuel, M. Endler, B. A. Carreras, and D. E. Newman, Phys. Plasmas **7**, 1408 (2000).

[14]G. Y. Antar, P. Devynck, X. Garbet, and S. C. Luckhardt, Phys. Plasmas **8**, 1612 (2001).
[15]R. Barni and C. Riccardi, Plasma Phys. Controlled Fusion **51**, 085010 (2009).
[16]M. A. Pedrosa, C. Hidalgo, B. A. Carreras, R. Balbín, I. García-Cortés, D. Newman, B. van Milligen, E. Sánchez, J. Bleuel, M. Endler, S. Davies, and G. F. Matthews, Phys. Rev. Lett. **82**, 3621 (1999).
[17]A. A. Ferreira, M. V. A. P. Heller, I. L. Caldas, E. A. Lerche, L. F. Ruchko, and L. A. Baccalá, Plasma Phys. Control. Fusion **46**, 669 (2004).
[18]T. Uckan, B. Richards, R. D. Bengtson, B. A. Carreras, G. Li, P. D. Hurwitz, W. L. Rowan, H. Y. W. Tsui, and A. J. Wootton, Nucl. Fusion **35**, 487 (1995).
[19]C. Hidalgo, C. Alejaldre, A. Alonso, J. Alonso, L. Almoguera, F. de Aragon, E. Ascasıbar, A. Baciero, R. Balbın, E. Blanco, J. Botija, B. Brañas, E. Calderon, A. Cappa, J. A. Carmona, R. Carrasco, F. Castejon, J. R. Cepero, A. A. Chmyga, J. Doncel, N. B. Dreval, S. Eguilior, L. Eliseev, T. Estrada, J. A. Ferreira, A. Fernandez, J. M. Fontdecaba, C. Fuentes, A. Garcıa, I. Garcıa-Cortes, B. Gonc¸alves, J. Guasp, J. Herranz, A. Hidalgo, R. Jimenez, J. A. Jimenez, D. Jimenez- Rey, I. Kirpitchev, S. M. Khrebtov, A. D. Komarov, A. S. Kozachok, L. Krupnik, F. Lapayese, M. Liniers, D. Lopez-Bruna, A. Lopez-Fraguas, J. Lopez-Razola, A. Lopez-Sanchez, E. de la Luna, G. Marcon, R. Martan, K. J. McCarthy, F. Medina, M. Medrano, A. V. Melnikov, P. Mendez, B. van Milligen, I. S. Nedzelskiy, M. Ochando, O. Orozco, J. L. de Pablos, L. Pacios, I. Pastor, M. A. Pedrosa, A. de la Peña, A. Pereira, A. Petrov, S. Petrov, A. Portas, D. Rapisarda, L. Rodrıguez-Rodrigo, E. Rodrıguez-Solano, J. Romero, A. Salas, E. Sanchez, J. Sanchez, M. Sanchez, K. Sarksian, C. Silva, S. Schchepetov, N. Skvortsova, F. Tabares, D. Tafalla, A. Tolkachev, V. Tribaldos, I. Vargas, J. Vega, G. Wolfers, and B. Zurro, Nucl. Fusion **45**, S266 (2005).
[20]G. Van Oost, J. Adamek, V. Antoni, P. Balan, J. A. Boedo, P. Devynck, I. Duran, L. Eliseev, J. P. Gunn, M. Hron, C. Ionita, S. Jachmich, G. S. Kirnev, E. Martines, A. Melnikov, R. Schrittwieser, C. Silva, J. Stöckel, M. Tendler, C. Varandas, M. Van Schoor, V. Vershkov, and R. R. Weynants, Plasma Phys. Controlled Fusion **45**, 621 (2003).
[21]I. C. Nascimento, Y. K. Kuznetsov, J. H. F. Severo, A. M. M. Fonseca, A. Elfimov, V. Bellintani, M. Machida, M. V. A. P. Heller, R. M. O. Galvao, E. K. Sanada, and J. I. Elizondo, Nucl. Fusion **45**, 796 (2005).
[22]K. W. Gentle and H. He, Plasma Sci. Technol. **10**, 284 (2008).
[23]K. Rypdal and S. Ratynskaia, Phys. Rev. Lett. **94**, 225002 (2005).
[24]P. Ricci, B. N. Rogers, and S. Brunner, Phys. Rev. Lett. **100**, 225002 (2008).
[25]S. H. Miller, A. Fasoli, B. Labit, M. McGrath, O. Pisaturo, G. Plyushchev, M. Podesta, and F. M. Poli, Phys. Plasmas **12**, 090906 (2005).
[26]F. J. Øynes, O. M. Olsen, H. L. Pecseli, A. Fredriksen, and K. Rypdal, Phys. Rev. E **57**, 2242 (1998).
[27]S. Luckhardt, "The Helimak: A one dimensional toroidal plasma system," Technical Report No. UCSD-ENG-069, University of California, San Diego, 1999.
[28]K. W. Gentle, K. Liao, K. Lee, and W. L. Rowan, Plasma Sci. Technol. **12**, 391 (2010).
[29]J. C. Perez, W. Horton, K. W. Gentle, W. L. Rowan, K. Lee, and R. B. Dahlburg, Phys. Plasmas **13**, 032101 (2006).
[30]D. L. Toufen, Z. O. Guimarães-Filho, I. L. Caldas, F. A. Marcus, and K. W. Gentle, Phys. Plasmas **19**, 012307 (2012).
[31]D. L. Toufen, Z. O. Guimarães-Filho, I. L. Caldas, J. D. Szezech, S. Lopes, R. L. Viana, and K. W. Gentle, Phys. Plasmas **20**, 022310 (2013).
[32]P. Devynck, G. Antar, G. Wang, X. Garbet, J. Gunn, and J. Y. Pascal, Plasma Phys. Controlled Fusion **42**, 327 (2000).
[33]B. Labit, I. Furno, A. Fasoli, A. Diallo, S. H. Muller, G. Plyushchev, M. Podestà, and F. M. Poli, Phys. Rev. Lett. **98**, 255002 (2007).
[34]Z. O. Guimarães-Filho, I. L. Caldas, R. L. Viana, I. C. Nascimento, Yu. K. Kuznetsov, and J. Kurths, Phys. Plasmas **17**, 012303 (2010).
[35]T. Levinson, J. M. Beall, E. J. Powers, and R. D. Bengtson, Nucl. Fusion **24**, 527 (1984).
[36]Ch. P. Ritz, E. J. Power, T. L. Rhodes, R. D. Bengtson, K. W. Gentle, H. Lin, P. E. Phillips, A. J. Wootton, D. L. Brower, N. C. Luhmann, Jr., W. A. Peebles, P. M. Schoch, and R. L. Hickok, Rev. Sci. Instrum. **59**, 1739 (1988).
[37]G. Boffetta, V. Carbone, P. Giuliani, P. Veltri, and A. Vulpiani, Phys. Rev. Lett. **83**, 4662 (1999).
[38]J. H. Yu, C. Holland, G. R. Tynan, G. Antar, and Z. Yan, J. Nucl. Mater. **363**, 728 (2007).
[39]E. G. Garcia, Phys. Rev. Lett. **108**, 265001 (2012).
[40]I. Furno, B. Labit, M. Podestà, A. Fasoli, S. H. Müller, F. M. Poli, P. Ricci, C. Theiler, S. Brunner, A. Diallo, and J. Graves, Phys. Rev. Lett. **100**, 055004 (2008).
[41]C. Theiler, A. Diallo, A. Fasoli, I. Furno, B. Labit, M. Podestà, F. M. Poli, and P. Ricci, Phys. Plasmas **15**, 042303 (2008).
[42]C. Theiler, I. Furno, J. Loizu, and A. Fasoli, Phys. Rev. Lett. **108**, 065005 (2012).